FACULTY OF ELECTRICAL ENGINEERING
KTE
September 10 - 12, 2007
Pilsen, Czech Republic

OPERATION PARAMETERS AND CHARACTERISTICS OF ACTUATORS WITH DILATATION ELEMENT

IVO DOLEŽEL[1], PAVEL KARBAN[2], BOHUŠ ULRYCH[2], JERZY BARGLIK[3]
MYKHAILO PANTELYAT[4], YURI MATYUKHIN[4], PAVLO GONTAROWSKIY[4]

Abstract: ***In specific applications one needs actuators characterized by very high forces at small shifts. As actuators of classical constructions mostly cannot satisfy these requirements, the authors designed another arrangement with an inductively heated dilatation element. But huge mechanical strains and stresses of thermoelastic origin acting in its structural parts could lead to its damage or destruction. The paper deals with mathematical modeling of the device that is solved numerically in the combined formulation (while the electromagnetic field is solved independently, the thermal and thermoelastic effects are solved in the hard-coupled formulation). The algorithm is illustrated on a typical example whose results are discussed.***

Key words: *actuator, numerical analysis, electromagnetic field, temperature field, field of thermoelastic displacements.*

INTRODUCTION

Electromechanical actuators (force elements, electromechanical converters) are devices converting the effects of the electric current into the mechanical forces or torques. They are widely employed in various industrial and transport plants and also in the technological processes of automated production systems. The function of an actuator can be derived from various physical principles. Well known and widely used are, for example, the ferromagnetic actuators based on the magnetic force of an electromagnet. But in specific applications requiring generation of high forces at small shifts, the actuators of classical constructions usually fail. For such purposes one can use thermoelastic actuators based on the thermal dilatation of metals or unequal dilatability of two different metals that are mechanically connected and electrically heated. These devices are typically used as fixing elements in working lines with numerically controlled machine tools.

The authors proposed several types of an actuator working with an inductively heated dilatation element. The paper deals with its mathematical model and its solution with the aim to find the operation parameters and characteristics of the device. The methodology is illustrated on an example whose results are discussed.

1 FORMULATION OF THE PROBLEM

The principal scheme of this fixing device is in Fig. 1. Its basic part is a dilatation (usually inductively heated) element **1** with a source of heat **2**. On one part the dilatation element is fixed to a stiff wall **3** with which it is shifted to the fixed body **4** that is also considered stiff. The system is assumed to be in the force equilibrium characterized by a compressing force $\boldsymbol{F}_c$ between the body and dilatation element that fixes the body **4** in the given position.

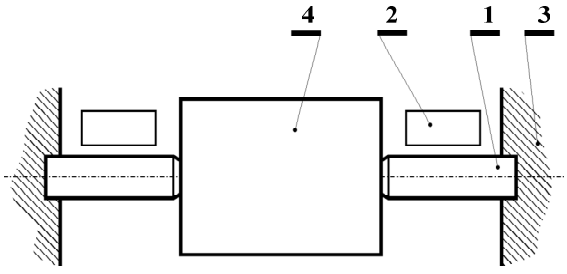

Fig. 1: The principal scheme of employment of the thermoelastic actuator
1 – heated dilatation element, **2** – source of heat, **3** – stiff wall, **4** – fixed body

The fundamental condition of successful operation of the actuator is the fastest possible and most economical heating of the dilatation element **1**. In case of the induction heating it requires to arrange the actuator in such a manner that allows converting as much electromagnetic energy (delivered by the field coil carrying current I_{ext})

into the internal energy of the dilatation element as possible. The ratio of this internal energy is the temperature of the element **1**. Evaluation of several possible arrangements of the actuator with respect to the above condition is one of the fundamental aims of the paper.

Analyzed are four variants of an axially symmetric arrangement of the thermoelastic monometallic actuator, see Fig. 2a, b, c, d.

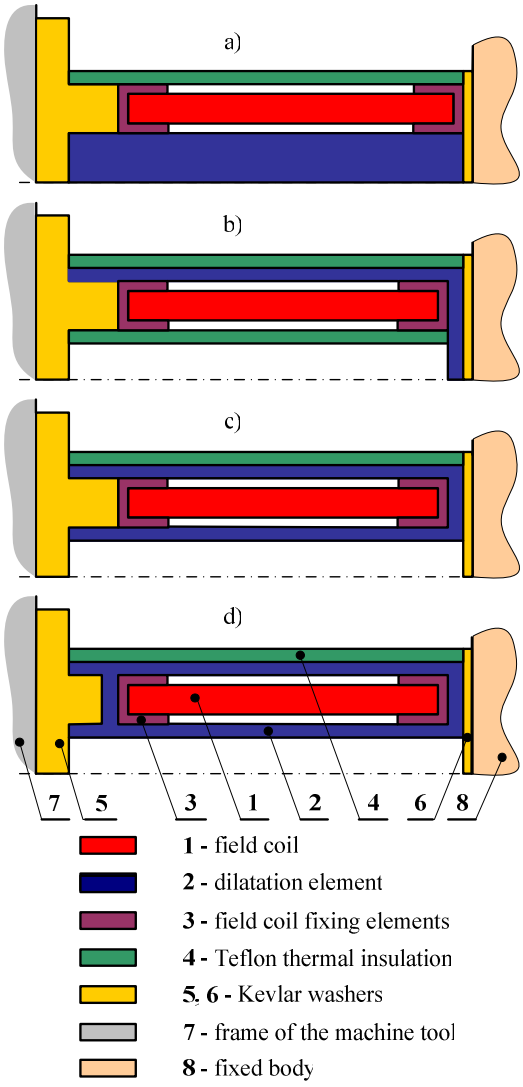

Fig. 2a, b, c, d: Four variants of the investigated actuator

The dilatation element **2** (a cylinder, tube or a system of two coaxial tubes) is fixed into a stiff insulating flange washer (Kevlar) **5** that is fixed to the solid frame of the machine tool **7**. The insulation shell **4** (that is also fixed to the flange washer **5**) contains two elements **3** fixing the field coil **1**. The field coil carries harmonic current of the amplitude I_v and frequency f. This current generates a time variable magnetic field that warms up the dilatation element **1** by induction. Due to its heating and consequent thermal dilatation the element **2** pulls through the solid insulating washer **6** on the fixed body **8** by force $\boldsymbol{F}_c$. The closer is the dilatation element **2** to the fixed body **8** at the beginning of the process of heating and the higher is its temperature, the higher is this force. It is also clear that the electromagnetic energy accumulated in the dilatation element **2** (and, consequently, the force $\boldsymbol{F}_c$) depends on the overall arrangement of the actuator, particularly on the mutual position of the coil **1** and dilatation element **2**.

The aim of the paper was to determine the

- optimal arrangement of the actuator from the viewpoint of accumulation of the electromagnetic energy in the dilatation element **2** for four technologically acceptable variants depicted in Figs. 2a, b, c, d.
- static characteristic of the actuator, i.e. the dependence of its fixing force $\left|\boldsymbol{F}_c\left(d_0\right)\right|$ on the amplitude I_v of the field current (d_0 being the thickness of the air gap between the touching surface of the washer **6** and fixed body before heating)
- the dependence of the fixing force $\left|\boldsymbol{F}_c\left(d_0\right)\right|$ on frequency f of the field current for a given value of the distance d_0.

Solution to the problem is carried out as a weakly coupled problem formulated in the cylindrical coordinate system (r, φ, z). This coupling includes

- harmonic electromagnetic field,
- stationary temperature field,
- field of the thermoelastic displacements.

2 MATHEMATICAL MODEL OF THE PROBLEM

2.1. Harmonic electromagnetic field

The definition area of the problem consisting of seven subregions is depicted in Fig. 3 (compare also with Fig. 2d). The area is bounded by the fictitious boundary $A_E B_E C_E D_E$.

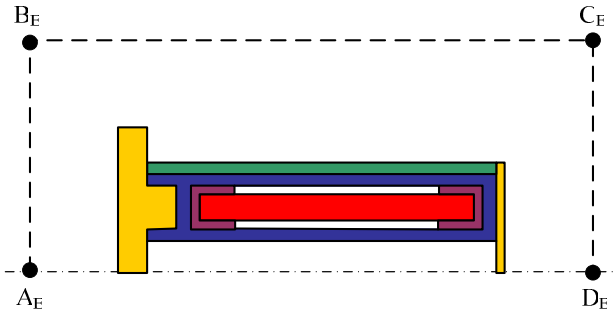

Fig. 3: The definition area of the electromagnetic field (device of type d, see Fig. 2)

Distribution of the electromagnetic field in space and time is (because of the presence of nonlinearities) described by the solution of the well-known parabolic differential equation for the magnetic vector potential $\boldsymbol{A}$ in the form [1]

$$\operatorname{curl}\left(\frac{1}{\mu}\operatorname{curl}\boldsymbol{A}\right)+\gamma\frac{\partial \boldsymbol{A}}{\partial t}=\boldsymbol{J}_{\text{ext}} \qquad (1)$$

where μ denotes the magnetic permeability, γ the electric conductivity and $\boldsymbol{J}_{\text{ext}}$ the vector of the uniform external harmonic current density in the field coil.

But solution to this equation is, in this case, practically unfeasible due to relatively long time of the process of

heating. That is why the model was linearized, so that the magnetic field could be considered harmonic. Then it can be described by the Helmholtz equation for the phasor $\underline{\boldsymbol{A}}$ of the magnetic vector potential $\boldsymbol{A}$

$$\mathrm{curlcurl}\,\underline{\boldsymbol{A}} + \mathrm{j}\cdot\omega\gamma\mu\,\underline{\boldsymbol{A}} = \mu\underline{\boldsymbol{J}}_{\mathrm{ext}}\,. \tag{2}$$

The numerical solution to this equation can be, however, carried out iteratively; the permeability μ in all elements containing ferromagnetic material is always adjusted to the real value of the corresponding magnetic flux density.

In fact, the real solution presented in the paper is a compromise. The region containing the ferromagnetic material (dilatation cylinder **2**) was divided into several subregions whose permeabilities were considered constant. And they were recalculated at each iteration step as the average values of the permeability in the relevant subregion.

This simplification is also advantageous from the viewpoint of determining the distribution of the specific losses w representing the internal sources of heat in the ferromagnetic dilatation cylinder **2**. These losses are considered as a sum of the specific Joule losses w_{J} and magnetization losses w_{m}, so that

$$w = w_{\mathrm{J}} + w_{\mathrm{m}} \tag{3}$$

where

$$w_{\mathrm{J}} = \frac{\left|\underline{\boldsymbol{J}}_{\mathrm{eddy}}\right|^2}{\gamma}, \quad \underline{\boldsymbol{J}}_{\mathrm{eddy}} = \mathrm{j}\cdot\omega\underline{\boldsymbol{A}} \tag{4}$$

while w_{m} are determined from the known measured loss dependence $w_{\mathrm{m}} = w_{\mathrm{m}}\left(\left|\underline{\boldsymbol{B}}\right|\right)$ for the used material (magnetic flux density $\boldsymbol{B}$ in every element is also harmonic).

As far as the arrangement of the actuator may be considered axisymmetric, the magnetic vector potential $\boldsymbol{A}$ and current densities $\boldsymbol{J}$ have only one nonzero component in the circumferential direction $\boldsymbol{\varphi}_0$. This leads to an essential simplification of the previous equations.

The boundary conditions along the axis of the arrangement and artificial boundary $\mathrm{A_E B_E C_E D_E}$ placed at a sufficient distance from the system are of the Dirichlet type. The corresponding equation reads $\underline{A}_{\varphi}(r,z) = 0$.

2.2. Stationary temperature field

The definition area of the problem consisting of seven subregions is depicted in Fig. 4 (compare with Fig. 2d). The area is bounded by the line $\mathrm{A_T B_T C_T D_T A_T}$.

The differential equation describing the distribution of the steady-state temperature reads [2]

$$\mathrm{div}\left(\lambda\cdot\mathrm{grad}T\right) = -w \tag{5}$$

where λ is the thermal conductivity and w are the internal sources of heat given by (3).

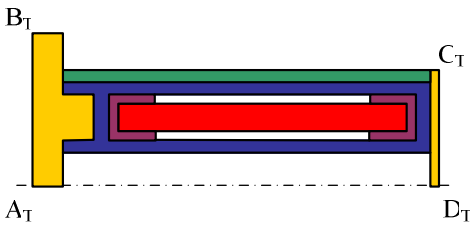

Fig. 4: The definition area of the temperature field (device of type d, see Fig. 2)

The boundary conditions securing the uniqueness of the solution of (5) may be expressed in the form (in accordance with Fig. 4)

- axis $\mathrm{A_T D_T}$: $\dfrac{\partial T}{\partial n} = -\dfrac{\partial T}{\partial r} = 0$ (rotational symmetry),
- line $\mathrm{C_T D_T}$: $T = T_{\vartheta}$ (contact with the fixed body **8** of temperature ϑ),
- line $\mathrm{B_T C_T}$: $-\lambda\dfrac{\partial T}{\partial n} = \alpha\left(T - T_{\mathrm{a}}\right)$ (contact with the ambient air of temperature T_{a}),
- line $\mathrm{A_T B_T}$: $T = T_{\mathrm{s}}$ (contact with the solid frame **7** of the machine tool of temperature T_{s}).

2.3. Field of thermoelastic displacements

The definition area of the problem consists of one region corresponding to the dilatation element **2** (see Fig. 2d). This region is bounded by the line $\mathrm{A_S B_S C_S D_S A_S}$, see Fig. 5.

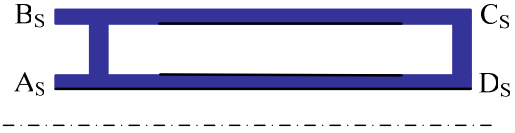

Fig. 5: The definition area of the field of thermoelastic displacements (device of type d, see Fig. 2)

The Lamé equations describing the field of thermoelastic displacements $\boldsymbol{u}(r,z)$ due to the distribution of the steady-state temperature field $T(r,z)$ read [3]

$$\begin{aligned}&(\varphi+\psi)\cdot\mathrm{grad}\left(\mathrm{div}\,\boldsymbol{u}\right)+\psi\cdot\Delta\boldsymbol{u}-\\&-(3\varphi+2\psi)\cdot\alpha_{\mathrm{T}}\cdot\mathrm{grad}\,T+\boldsymbol{f}=\boldsymbol{0},\end{aligned} \tag{6}$$

where $\varphi \geq 0, \psi > 0$ are coefficients associated with material parameters by relations

$$\varphi = \frac{\nu\cdot E}{(1+\nu)(1-2\nu)}, \quad \psi = \frac{E}{2\cdot(1+\nu)} \tag{7}$$

where E is the modulus of elasticity and ν the Poisson coefficient of the transverse contraction. Finally α_{T} denotes the coefficient of linear thermal dilatability and $\boldsymbol{f}$ the vector of the internal volume forces.

The displacements were calculated in the dilatation

element **2** for $\boldsymbol{f} = \mathbf{0}$. The knowledge of the displacement is the starting point for finding the corresponding deformations. These can be calculated (in cylindrical coordinate system r, z, φ) from formulas

$$\varepsilon_{rr} = \frac{\partial u_r}{\partial r},\ \varepsilon_{\varphi\varphi} = \frac{u_r}{r} + \frac{1}{r}\cdot\frac{\partial u_\varphi}{\partial \varphi},\ \varepsilon_{zz} = \frac{\partial u_z}{\partial z},$$
$$\varepsilon_{rz} = \frac{1}{2}\left(\frac{\partial u_r}{\partial z} + \frac{\partial u_z}{\partial r}\right). \tag{8}$$

Using the Hook law in the tensorial form we finally calculate the corresponding strains and stresses σ_{rr}, $\sigma_{\varphi\varphi}$, σ_{zz} and σ_{rz} in the element **2**.

The axial component $F_{c,z}$ of the total compressing force $\boldsymbol{F}_c$ acting by the dilatation element in the direction of axis z on the fixed body **8** then follows from the integration of the relevant axial stresses over its cross-section. There holds

$$F_{c,z} = \iint_{S_{28}} \sigma_{zz}\,\mathrm{d}S, \tag{9}$$

where σ_{zz} denotes the distribution of the axial stresses and S_{28} is the contact area between the element **2** and fixed body **8**.

The boundary conditions follow from the condition of fixing between the frame **7** of the machine tool and fixed body **8**. There holds

- line $A_S B_S$: $u_z = 0$ (contact with the solid frame **7** of the machine tool).
- line $C_S D_S$: $u_z = 0$ (contact with the fixed body **8**),
- other parts of the boundary: no conditions (free surface).

3 COMPUTER MODEL AND ACCURACY OF SOLUTION

The mathematical model described in the previous paragraph was solved by the FEM-based code QuickField [4] supplemented with a number of procedures developed and written by the authors. Special attention was paid to the convergence of the results in dependence on the density of the discretization meshes and, for the electromagnetic field also in dependence on the position of the artificial external boundary $A_E B_E C_E D_E$. Tab. 1 shows the number of nodes necessary for reaching results with three valid digits for the actuator of type d) that has the best operation parameters.

Tab. 1: The number of nodes necessary for reaching accuracy on 3 valid digits

	field		
	elmag.	temp.	thermoel.
quantity	w (W/m^3)	T (°C)	$\boldsymbol{u}$ (m)
nodes	116 043	32 954	17 594

4 ILLUSTRATIVE EXAMPLE

4.1. The technical setup

We consider four variants of a rotationally symmetrical arrangement of the thermoelastic monometallic actuator:

- variant a) (see Fig. 2a) with the dilatation element **2** in the shape of a full cylinder (a traditional arrangement),
- variant b) (see Fig. 2b) with the dilatation element **2** in the shape of a pipe framed to the field coil **1**,
- variant c) (see Fig. 2c) with the dilatation element **2** in the shape of two coaxial pipes connected by a front with the field coil **1** inserted between them,
- variant d) (see Fig. 2d) with the dilatation element **2** in the shape of two coaxial pipes connected by two fronts at both ends with the field coil **1** inserted inside this structure.

Given are all geometrical dimensions (for the variant d), for example, in Fig. 6) and physical properties of all materials used – see Tab. 2a, b.

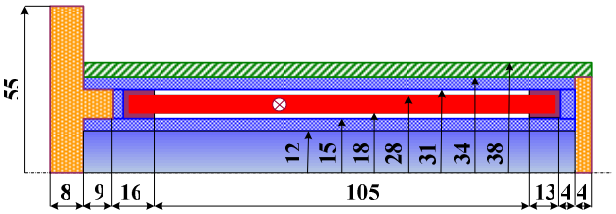

Fig. 6: The geometrical dimensions of the device of the type d, see Fig. 2

Tab. 2a: The electrical and thermal parameters of particular subregions

element	material	γ	μ_r	λ
		MS/m	–	W/mK
1	Cu	57	1	390
2	steel 12 040	1.5	$B(H)$	$\lambda(T)$
3	Teflon	0	1	1.6
4	Teflon	0	1	1.6
5	Kevlar *	0	1	0.04
6	Kevlar *	0	1	0.04
7	air	0	1	0.042

dependence $B(H)$: see Fig. 7

dependence $\lambda(T)$: see Fig. 8

* see [6], Kevlar TVARON

Tab. 2b: The mechanical parameters of particular subregions

element	material	E	ν	α_T
		N/m^2	–	1/K
1	Cu		-	-
2	steel 12 040	$2.1\cdot10^{11}$	0.3	$1.25\cdot10^{-5}$
3	Teflon	0	-	-
4	Teflon	0	-	-
5	Kevlar	$1.24\cdot10^{11}$	0.3	$2\cdot10^{-6}$
6	Kevlar	$1.24\cdot10^{11}$	0.3	$2\cdot10^{-6}$
7	air	-	-	-

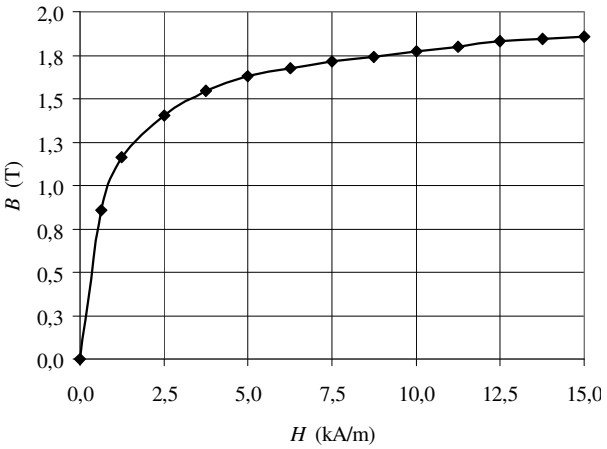

Fig. 7: The magnetization characteristic of steel 12 040

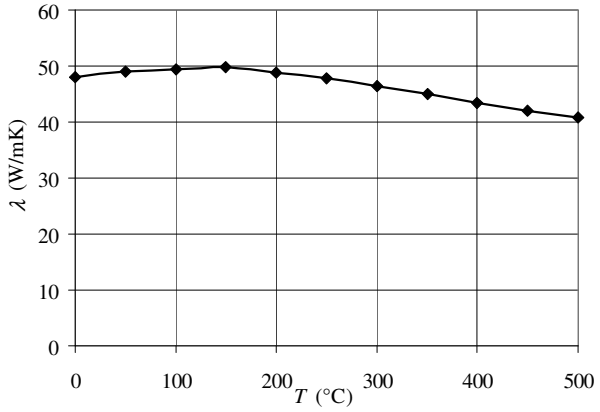

Fig. 8: The thermal conductivity versus temperature for steel 12 040

The field coil **1** containing $N_z = 1250$ turns from a Cu conductor of diameter $D_c = 1$ mm (the factor of filling $\kappa = 0.785$) carries current I_v of frequency f (see Figs. 14 and 15) with corresponding current density $J_v \approx J_{ext}$ (see also equation (1) or Tab. 3). The dilatation element 2 is made from the carbon steel 12 040 whose dependencies $B(H)$ and $\lambda(T)$ are shown in Figs. 7 and 8.

The aim of the computations is to find the most advantageous arrangement of the device (see Figs. 2a – 2d) and evaluate its basic properties, particularly its static characteristic, i.e. the dependence of the fixing force $F_c(d_2 / d_{max})$ on the field current I_v and its frequency f . Here

- d_2 denotes the thickness of the air gap between the contact surface between the dilatation element **2** and fixed body **8** before the beginning of fixing,
- d_{max} is the maximal thermal dilatation of element **2** provided that the dilatation is not prevented.

4.2. Results and their discussion

The basic evaluation of the devices can be performed from the comparison of magnetic fields generated by particular arrangement. The corresponding maps are shown in Figs. 9a–9d.

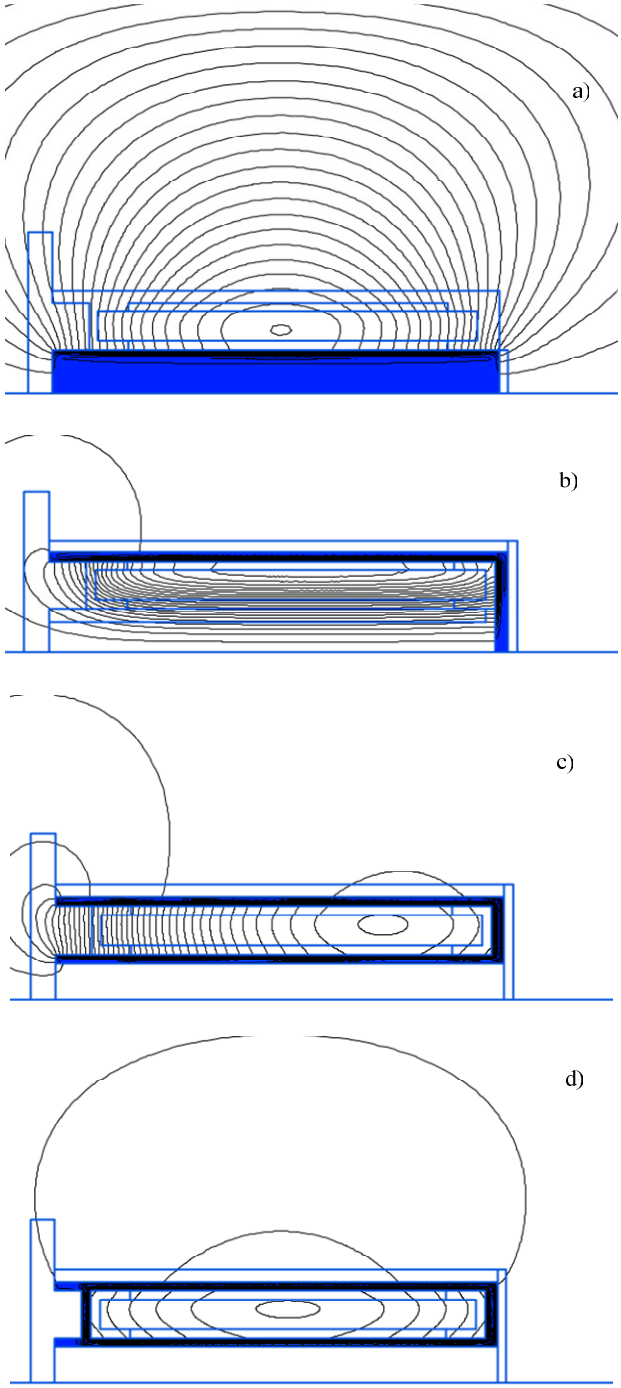

Fig. 9: Maps of the magnetic field in particular variants a)–d) of the thermoelastic actuator (see Fig. 2)

It is clear that from the viewpoint of the magnetic field distribution is the variant d). Here the leakage of the force lines is very small (when compared with other dispositions), so that in this case we can expect the best utilization of the magnetic field energy for heating of the dilatation element **2**.

This conclusion follows even from Tab. 3 containing the comparison of all basic parameters of the mentioned variants. Important are mainly these values:

- the maximal compressing force $|F_{c,max}|$ for the case when $d_2 = 0$ (perfect contact between the dilatation element **2** and fixed body **8**),
- the maximal thermal dilatation d_{max} .

Tab. 3: Comparison of the principal parameters of the investigated variants of the actuator ($J_{ext} = 2 \cdot 10^6$ A/m^2, $f = 50$ Hz)

quantity	arrangement (see Fig. 2)			
	a)	b)	c)	d)
volume of the dilatation element **2** (m^3)	1.039E-4	1.179E-4	1.367E-4	1.367E-4
total losses (W)	1.385E1	1.951E1	1.093E1	1.924E2
specific losses (W/m^3)	1.333E5	1.655E3	7.996E5	1.339E6
average temperature of the element **2** (°C)	6.658E1	2.104E1	1.523E2	2.584E2
average temperature of the coil **1** (°C)	5.521E1	2.116E1	1.531E2	2.598E2
maximal thermal dilatation (m)	8.480E-5	1.820E-6	8.150E-5	4.340E-4
maximal force (N) *	8.847E4	2.196E3	1.211E5	6.180E5
reduced stress (N/m^2)	4.020E8	1.120E7	4.781E8	2.590E9

* only theoretical values provided that the fixed body is perfectly stiff

The following Figs. 10–12 illustrate the basic properties of the actuator of the optimal type d).

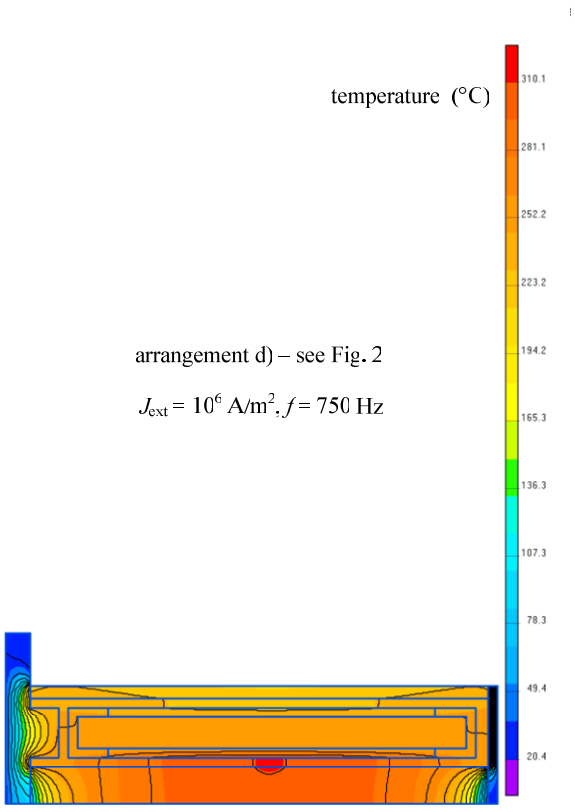

Fig. 10: The temperature map in the system

Fig. 10 shows the distribution of the steady-state temperature field for $J_{ext} = 10^6$ A/m^2, $f = 750$ Hz). It is clear that the temperature field in the dilatation element **2** is almost uniform, with slightly higher temperatures in its internal part. This is advantageous from the viewpoint of its primary thermoelastic strains and stresses.

Figs. 11a and b contain qualitative information about the thermoelastic dilatations of the element **2**, again in the arrangement d), for both the free dilatation and for stiff contact between this element and fixed body **8**. The figures also show the reduced stresses according to the van Mises hypothesis. It is clear that these stresses are quite acceptable (there is no danger of irreversible plastic changes).

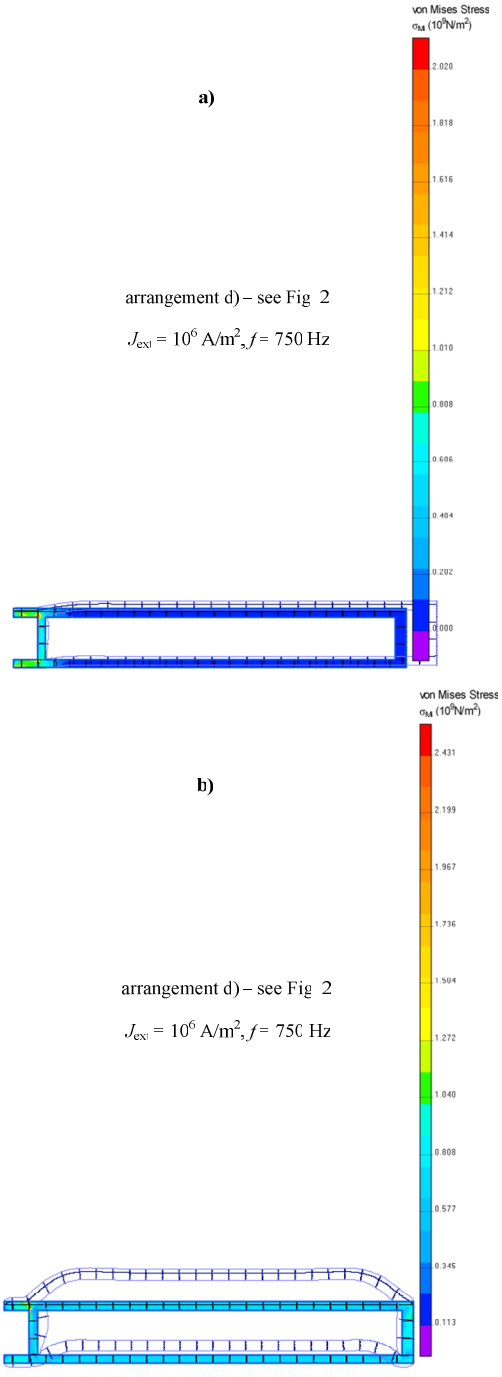

*Fig. 11: The thermoelastic displacements in element **2** (qualitative information)*
***a)** free dilatation, **b)** absolutely stiff fixed body*

Figs. 12a and b contains quantitative information about the thermoelastic displacements of the element **2**, again for both the free dilatation and for stiff contact between this element and fixed body **8**. It is clear that

- the dilatation in the axial direction reaches more than 0.4 mm, which is more that can provide analogous thermoplastic actuators of the classical type,
- the maximal dilatation in the radial direction is smaller than 0.13 mm, which is quite acceptable even from the technological viewpoint.

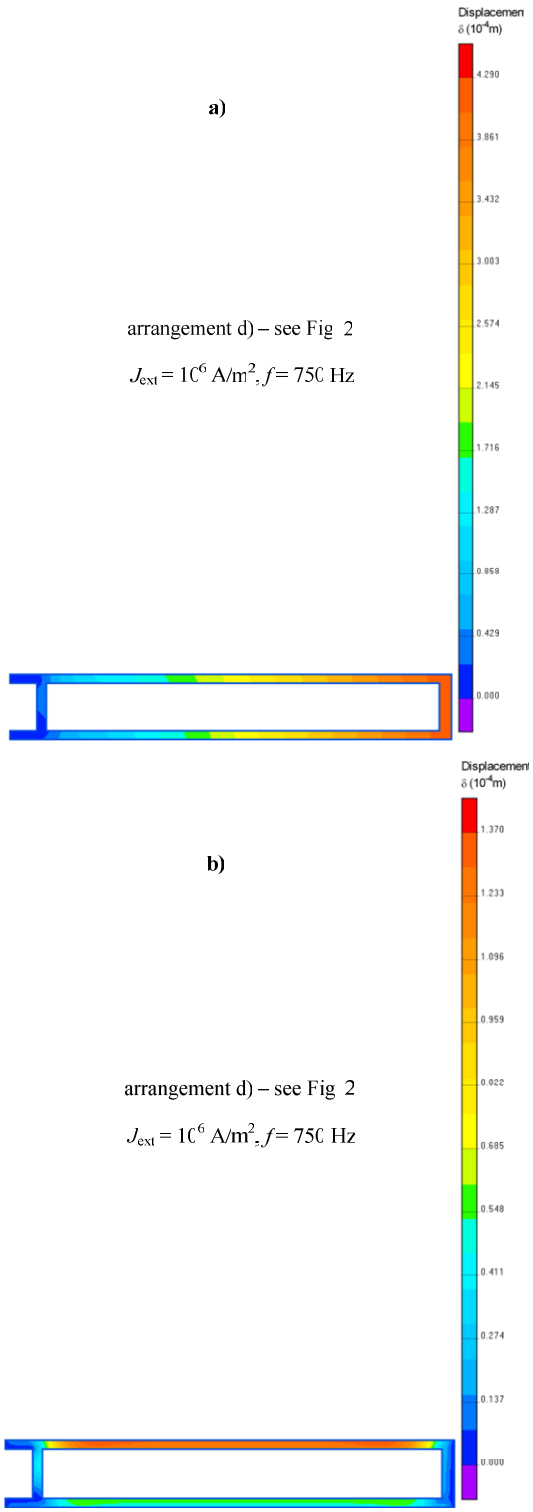

*Fig. 12: The thermoelastic displacements in element **2** (quantitative information)*
***a)** free dilatation, **b)** absolutely stiff fixed body*

The static characteristics of the optimal arrangement of type d) (see Fig. 2) as functions of the current I_v and frequency f are in Figs. 13a and b. The dependence of the compressing force $\boldsymbol{F}_c$ on parameter d_2 is practically linear and obviously can be modified in a wide range by selection of suitable values of I_v and f. On the other hand, from the viewpoint of operation of the device it would be better when the force $\boldsymbol{F}_c$ would be independent on the parameter d_2 as much as possible.

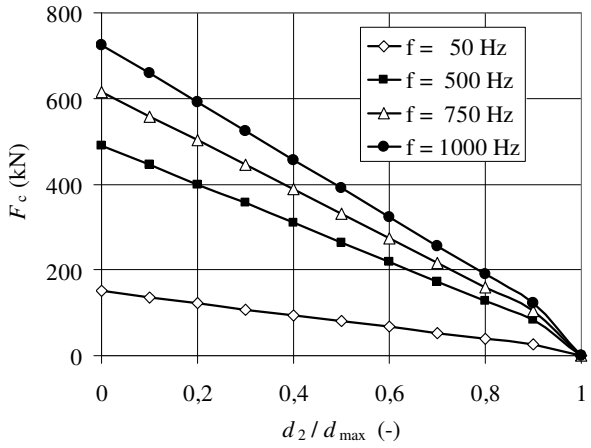

Fig. 13a: The static characteristic of the arrangement d) (the influence of the frequency f)

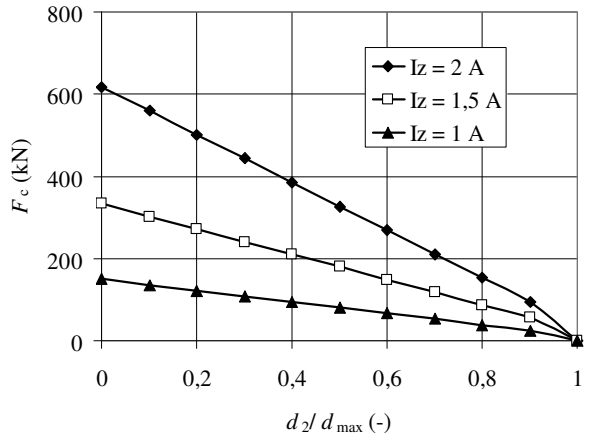

Fig. 13b: The static characteristic of the arrangement d) (the influence of the field current amplitude)

Other parameters concerning the actuator in arrangement d) can be found in Tabs. 4a and 4b. It can easily be deduced the particular influences of varying parameters of the field current.

5 CONCLUSION

The paper shows that relatively simple computation tools allow obtaining complete information about the operation parameters and characteristics of thermoelastic actuators. The most important quantity is the total compressing force $\boldsymbol{F}_c$ and its dependence various parameters of the device.

Next work in the field will be aimed at the:

- Possibility of increase of the force $\boldsymbol{F}_c$ using a longer

dilatation element **2** (see Fig. 2). In such a case it is necessary, however, to check the stiffness of this element and its stability with respect to its buckling (as in case of a unilaterally fixed beam of a ring cross-section).

- Suppression of the steepness of the static characteristic $\boldsymbol{F}_{\mathrm{c}}\left(d_2 / d_{\max}\right)$ of these actuators (compare Figs. 13 and 14) that is undesirable from the viewpoint of their operation.

Tab. 4a: The principal parameters of the actuator of type d) for changing amplitude of the field current

quantity	value		
frequency (Hz)	50	50	50
current (A)	2	1.5	1
current density (A/m^2)	2E6	1.5E6	1E6
total losses (W)	1.924E2	1.082E2	4.810E1
specific losses (W/m^3)	1.339E6	7.534E5	3.348E5
average temperature of the element **2** (°C)	2.584E2	1.488E2	7.773E1
average temperature of the coil **1** (°C)	2.598E2	1.496E2	7.812E1
maximal thermal dilatation (m)	4.340E-4	2.300E-4	1.030E-4
maximal force (N) *	6.180E5	3.339E5	1.496E5
reduced stress (N/m^2)	2.590E9	1,090E9	5.911E8

* only theoretical values provided that the fixed body is perfectly stiff

Tab. 4b: The principal parameters of the actuator of type d) for changing frequency of the field current

quantity	value		
frequency (Hz)	500	750	1000
current (A)	1	1	1
current density (A/m^2)	1E6	1E6	1E6
total losses (W)	1.593E2	2.001E2	2.356E2
specific losses (W/m^3)	1.109E6	1.393E6	1.641E6
average temperature of the element **2** (°C)	2.092E2	2.574E2	2.995E2
average temperature of the coil **1** (°C)	2.103E2	2.587E2	3.010E2
maximal thermal dilatation (m)	3.380E-4	4.250E-4	5.000E-4
maximal force (N) *	4.904E5	6.154E5	7.245E5
reduced stress (N/m^2)	1.940E9	2.431E9	2.861E8

* only theoretical values provided that the fixed body is perfectly stiff

6 ACKNOWLEDGMENT

Financial support of the Research Plan MSM6840770017, and Grant project GA CR 102/07/0496 is gratefully acknowledged.

7 REFERENCES

[1] Chari, M.V.K., Salon, S.J.: Numerical Methods in Electromagnetism. Academia Press, N.Y., 2000.
[2] Holman, J.P.: Heat Transfer, McGraw Hill Co., 2002.
[3] Boley, B.A, Wiener, J.H.: Theory of Thermal Stresses, NY, London, 1960.
[4] www.quickfield.com.
[5] Factory standard SKODA, SN 006004.
[6] www.azom.com.

Prof. Ing. Ivo Doležel, CSc.
Academy of Sciences of the Czech Republic
Institute of Thermomechanics
Dolejškova 5, 182 02 Praha 8
Czech Republic
E-mail: dolezel@iee.cas.cz

Ing. Pavel Karban, Doc. Ing. Bohuš Ulrych, CSc.
University of West Bohemia
Faculty of Electrical Engineering
Univerzitní 26, 306 14 Plzeň
Czech Republic
E-mail: {karban, ulrych}@kte.zcu.cz

Prof. dr. hab. Jerzy Barglik.
Silesian University of Technology
Department of Electrotechnology
Krasinskiego 8, 40-019 Katowice
Poland
E-mail: Jerzy.Barglik@polsl.pl

Ass. Prof. Pavlo Gontarovskiy, Ass. Prof. Yurii Matyukhin, Ass. Prof. Mykhailo Pantelyat
Institute of Problems in Machinery
National Ukrainian Academy of Sciences
Pozharsky str. 2/10, UA-61046 Kharkov
Ukraine
E-mail: shulzh@ipmach.kharkov.ua